J Fluoresc
DOI 10.1007/s10895-016-2020-z

ORIGINAL ARTICLE

Ni(II) and Zn(II) Complexes Containing Alkynyl Functionalized Salicylaldimine Ligand and Heterocyclic Coligand: Synthesis, Characterization and Luminescence Properties

M. S. More[1] · **S. S. Devkule**[1] · **S. S. Chavan**[1]

Received: 19 October 2016 / Accepted: 29 December 2016

Abstract Some nickel(II) and zinc(II) complexes of the type [Ni(**L**)(**phen**/**bipy**)]X (**1a–6a**) and [Zn(**L**)(**phen**/**bipy**)]X (**1b–6b**) (where **L** = 2-{(E)-[(4-trimethylsilylethynylphenyl)imino]methyl}-4-(4-nitro phenylethynyl)phenol; **phen** = 1, 10-phenanthroline, **bipy** = 2, 2′-bipyridine; X = ClO_4^-, BF_4^-, PF_6^-) have been prepared and characterized on the basis of elemental analyses, FTIR, ^1H NMR and mass spectral studies. The molecular structure of **L** was determined by single crystal X-ray diffraction studies. The electrochemical behaviour of the Ni(II) complexes indicate that the **phen** complexes appears at more positive potential as compared to those for **bipy** complexes, as a consequence of its strong π-acidic character. TGA was carried out to study the thermal behavior of the complexes. Room temperature luminescence is observed for all complexes corresponds to $\pi \rightarrow \pi^*$ ILCT transition. The size of the counter anion and heterocyclic coligands **phen** and **bipy** shows marked effect on emission properties of the complexes.

Keywords Schiff base · Ni(II)/Zn(II) complexes · Photoluminescence

Introduction

The rational design and construction of inorganic–organic hybrid materials made up of nitrogen/oxygen-donor ligands have attracted considerable attention owing to their intriguing architectures and topologies, as well as potential applications in many fields. Much effort has been focused on the synthesis and properties of transition metal complexes of hybrid ligands because they can provide new materials with useful properties such as magnetic exchange [1], electrical conductivity [2], photoluminescence [3], nonlinear optical property [4] and antimicrobial activity [5]. Among the various ligands Schiff bases are very interesting compounds because of their facile syntheses, easily tuneable steric, electronic properties and good solubility in common solvents [6, 7]; and also these are very important classes of organic compounds from both practical and theoretical point of view. Salicylaldimine Schiff base ligands containing N and O donor atoms in particular are interesting due to their ability to possess unusual configuration, structural lability and their sensitivity towards molecular environments [8]. They exhibit multifunctional properties such as non-linear optical (NLO) materials [9], supramolecular nanostructures [10], fluorescent molecular probes [11], molecular aggregates [12], optical probes for medical applications [13] and electron transporting materials [14]. In recent years considerable research efforts have been focused on incorporation of additional functionalities into coordinating ligand which are reported to exhibit very interesting luminescent and optical properties [15]. The incorporation of additional functionality into coordinating ligand and their metal complexes was found to destabilize non-radiative d-d transitions to maintain the structural integrity and thus displaying reasonable luminescence properties. In particular, addition of alkynyl functionality with π-conjugation constitutes an important class of compounds as a luminescent material due to their advanced electronic and structural properties [16, 17]. An important feature of this system is the structural modification which causes a large π-delocalization over the coordinated ligands than that of the regular complexes. The linear

---

✉ S. S. Chavan
sanjaycha2@rediffmail.com

[1] Department of Chemistry, Shivaji University, Kolhapur, MS 416 004, India

geometry of the alkynyl unit and its π-unsaturated nature has made them attractive for preparation of luminescent sensors, light emitting and nonlinear optical materials [18]. Moreover, rigidity of the structure and dipole moment of the complexes may thus increase. 1, 10-phenanthroline and 2, 2′-bipyridine chelators are also good nitrogen donors and the complexes formed serve as building blocks for the synthesis of metallodendrimers, supramolecular assemblies, in analytical chemisy, catalysis, electrochemistry, ring-opening metathesis and polymerization [19, 20]. They also act as potential antitumor agents and show better antitumor activity if they form neutral complexes with transition metal ions [21].

Influenced by these facts we report herein synthesis of some mixed ligand Ni(II) and Zn(II) complexes by the reaction of alkynyl functionalized salicylaldimine ligand 2-{(E)-[(4-trimethylsilylethynylphenyl)imino]methyl}-4-(4-nitrophenylethynyl)phenol (**L**) in presence of 1, 10 phenanthroline and 2, 2′-bipyridine as a coligand, All the complexes were characterized by elemental analyses and spectroscopic techniques. The influence of π-conjugation, coligands (**phen**, **bipy**) and size of the counter anion (ClO_4^-, BF_4^-, PF_6^-) on photophysical properties of the complexes have been studied.

Experimental

Materials and General Methods

Some manipulations were performed under nitrogen atmosphere using a vacuum line and standard Schlenk techniques. The CH_2Cl_2 was distilled from calcium hydride and diethyl ether and THF from Na-ketyl. All other solvents and reagents were of reagent grade and used without further purification. 5-ethynylsalicylaldehyde was prepared by following the procedure reported in the literature [22]. $Zn(BF_4)_2$ and $Zn(PF_6)_2$ were obtained by stirring $Zn(NO_3)_2.6H_2O$ with two equivalents of $NaBF_4$ and KPF_6 in acetonitrile at room temperature. The white solid ($NaNO_3$ or KNO_3) was filtered off, and the filtrate was evaporated to dryness to give the Zn(II) starting materials [23]. ^1H NMR spectra were recorded on Bruker 300 MHz instrument using TMS[$(CH_3)_4Si$] as an internal standard and were reported in units of δ with residual protons in the solvent as standard ($CDCl_3$, δ 7.24, d_6-dimethyl sulfoxide, δ 2.50). ESI mass spectra were recorded on JEOL SX-102 spectrometer. Elemental analyses (C, H and N) were performed on a Thermo Finnigan FLASH EA-112 CHNS analyzer. Absorption spectra were recorded on a Shimadzu UV–Vis–NIR-100 spectrophotometer. Luminescence properties were measured using a Perkin Elmer Spectroflourometer LS-55. Luminescence lifetime measurements were carried out by using time correlated single photon counting from HORIBA Jobin Yvon. Infrared spectra were recorded on a Perkin-Elmer FT-IR spectrometer using KBr pellets in the 4000–400 cm^{-1} spectral range. Cyclic voltammetry measurements were performed with CH-400A Electrochemical Analyzer. A standard three electrodes system consisting of Pt disk working electrode, Pt wire counter electrode and Ag/AgCl reference electrode was used. All the potentials were converted to SCE scale. Tetrabutylammonium perchlorate (TBAP) was used as the supporting electrolyte and all measurements were carried out in DMF solution at room temperature and scan rate 100 mV s^{-1}.

Synthesis

Synthesis of 5-(4-nitrophenyl)ethynylsalicylaldehyde

To a mixture of 1-iodo-4-nitrobenzene (1.310 g, 5.26 mmol), $Pd(PPh_3)_2Cl_2$ (0.074 g, 0.105 mmol), CuI (0.080 g, 0.42 mmol) in 30 ml of Et_3N, a 5 ml of 5-ethynylsalicylaldehyde (1.0 g, 6.84 mmol) in CH_2Cl_2 was added. The mixture was stirred for 16 h at 80 °C under N_2 atmosphere. The resulting mixture was filtered off and the residue obtained was purified by column chromatography on silica with CH_2Cl_2/Pet. ether (1:2) as an eluent. The yellow powder is afforded by removal of solvent under vacuum, and the product was identified as 5-(4-nitrophenyl)ethynylsalicylaldehyde.

Yield: 82%; Anal. Calcd for $C_{15}H_9NO_4$: C, 67.42; H, 3.39; 5.24. Found: C, 67.59; H, 3.47; N, 5.09; ^1H NMR ($CDCl_3$, 300 MHz): δ 11.22 (s, 1H, OH), 9.93 (s, 1H, HC = O), 8.23 (d, 1H, Ph), 7.82 (d, 1H, Ph), 7.71 (dd, 1H, Ph), 7.66 (dd, 2H, Ph), 7.04 (d, 1H, Ph); MS (EI): *m/z* 267 (M^+).

Synthesis of Ligand (L)

A solution of 4-(trimethylsilylethynyl)aniline (1 mmol, 0.189 g) in THF (10 ml) was added drop wise to a solution of 5-(4-nitrophenyl)ethynylsalicylaldehyde (1 mmol, 0.267 g) in THF (10 ml) with constant stirring. The resulting mixture was refluxed at about 80 °C until the completion of reaction (checked by TLC). The resulting solution was concentrated and the precipitate obtained was filtered, washed with diethyl ether and dried in vacuo.

Yield: 78%; Elemental analyses (C, H and N, wt%) Anal. Calc. for $C_{26}H_{22}N_2O_3Si$: C, 68.63; H, 5.51; N, 6.96; Found: C, 68.55; H, 5.39; N, 6.87; IR (KBr, cm^{-1}): 2203, υ(C ≡ C); 2155, υ(C ≡ CSi); 1618, υ(C = N); UV-Vis (DMF) λ_{max} (nm) (ε ×10^3, M^{-1} cm^{-1}): 231 (29.7.1), 265 (21.2), ^1H NMR ($CDCl_3$) (300 MHz): δ 13.29 (s, 1H, OH), δ 8.61 (s, 1H, HC = N), 7.98–6.65 (m, 11H, Ar-H), 0.27 (s, 9H, $(CH_3)_3Si$); MS (ESI): *m/z* 438 (M + Na).

Synthesis of Complex [Ni(L)(phen)]X (1a-3a)

To a solution of the appropriate Ni(II) salt, ((0.456 mmol, 0.1668 g), $Ni(ClO_4)_2{\cdot}6H_2O$; (0.456 mmol, 0.1552 g),

$Ni(BF_4)_2·6H_2O$ or (0.456 mmol, 0.1590 g), $Ni(PF_6)_2·6H_2O$) in THF (10 ml), an equimolar solution of ligand (**L**) (0.456 mmol, 0.200 g) in CH_2Cl_2 (20 ml) solution was added while stirring. The mixture was stirred for 20 min at room temperature. To this, a solution of one equivalent of 1, 10-phenanthroline (0.456 mmol, 0.0904 g) in THF (10 ml) was added with continuous stirring. The mixture was refluxed for 4 h. The precipitate obtained was filtered off, washed with diethyl ether and dried under vacuum.

1a: Yield: 78%; Elemental analyses (C, H and N, wt%) Anal. Calc. for $C_{38}H_{29}N_4O_7ClSiNi$: C, 58.82; H, 3.77; N, 7.22; Found: C, 58.75; H, 3.70; N, 7.29; IR (KBr, cm^{-1}): 2196, ν(C ≡ C); 2147, ν(C ≡ CSi); 1609, ν(C = N); 1097, 623, ν(ClO_4); UV-Vis (DMF) λ_{max} (nm) ($\varepsilon \times 10^3$, M^{-1} cm^{-1}): 235 (25.2), 274 (16.2), 373 (7.33), 525 (1.23); ^{1}H NMR (d_6-DMSO) (300 MHz): δ 8.65 (s, 1H, HC = N), 8.68–7.01 (m, 19H, Ar-H), 0.29 (s, 9H, $Si(CH_3)_3$); MS (ESI): 652 *m/z* (M-ClO_4)$^+$; **2a**: Yield: 81%; Elemental analyses (C, H and N, wt%) Anal. Calc. for $C_{38}H_{29}N_4O_3BF_4SiNi$: C, 59.80; H, 3.83; N, 7.34; Found: C, 59.72; H, 3.76; N, 7.41; IR (KBr, cm^{-1}): 2197, ν(C ≡ C); 2146, ν(C ≡ CSi); 1607, ν(C = N); 1071, ν(BF_4); UV-Vis (DMF) λ_{max} (nm) ($\varepsilon \times 10^3$, M^{-1} cm^{-1}): 244 (25.1), 276 (15.2), 376 (8.48), 536 (1.67); ^{1}H NMR (d_6-DMSO) (300 MHz): δ 8.64 (s, 1H, HC = N), 8.66–6.90 (m, 19H, Ar-H), 0.29 (s, 9H, $Si(CH_3)_3$); MS (ESI): *m/z* 652 (M-BF_4)$^+$; **3a**: Yield: 80%. Elemental analyses (C, H and N, wt%) Anal. Calc. for $C_{38}H_{29}N_4O_3PF_6SiNi$: C, 55.56; H, 3.56; N, 6.82; Found: C, 55.49; H, 3.48; N, 6.91; IR (KBr, cm^{-1}): 2194, ν(C ≡ C); 2144, ν(C ≡ CSi); 1606, ν(C = N); 845, 558, ν(P-F); UV-Vis (DMF) λ_{max} (nm) ($\varepsilon \times 10^3$, M^{-1} cm^{-1}): 245 (25.7), 277 (15.0), 370 (7.52), 529 (1.08); ^{1}H NMR (d_6-DMSO) (300 MHz): δ 8.65 (s, 1H, HC = N), 8.64–7.09 (m, 19H, Ar-H), 0.28 (s, 9H, $Si(CH_3)_3$); MS (ESI): *m/z* 652 (M-PF_6)$^+$.

Synthesis of Complex [Ni(L)(bipy)]X (4a-6a)

To a solution of the appropriate Ni(II) salt, ((0.490 mmol, 0.1793 g), $Ni(ClO_4)_2·6H_2O$; (0.490 mmol, 0.1669 g), $Ni(BF_4)_2·6H_2O$ or (0.490 mmol, 0.0874 g), $Ni(PF_6)_2·6H_2O$) in THF (10 ml), an equimolar solution of ligand (**L**) (0.490 mmol, 0.215 g) in CH_2Cl_2 (20 ml) solution was added while stirring. The mixture was stirred for 20 min at room temperature. To this, a solution of one equivalent of 2, 2′-bipyridine (0.490 mmol, 0.0765 g) in THF (10 ml) was added with continuous stirring. The mixture was refluxed for 4 h. The precipitate obtained was filtered off, washed with diethyl ether and dried under vacuum.

4a: Yield: 77%;. Elemental analyses (C, H and N, wt%) Anal. Calc. for $C_{36}H_{29}N_4O_7ClSiNi$: C, 57.51; H, 3.89; N, 7.45; Found: C, 57.46; H, 3.82; N, 7.53; IR (KBr, cm^{-1}): 2195, ν(C ≡ C); 2146, ν(C ≡ CSi); 1609, ν(C = N); 1096, 624, ν(ClO_4); UV-Vis (DMF) λ_{max} (nm) ($\varepsilon \times 10^3$, M^{-1} cm^{-1}): 242 (24.2), 275 (15.5), 359 (8.23), 518 (0.99); ^{1}H NMR (d_6-DMSO) (300 MHz): δ 8.64 (s, 1H, HC = N), 8.67–7.07 (m, 19H, Ar-H), 0.29 (s, 9H, $Si(CH_3)_3$), MS (ESI): *m/z* 652 (M-ClO_4)$^+$; **5a**:Yield: 80%; Elemental analyses (C, H and N, wt%) Anal. Calc. for $C_{36}H_{29}N_4O_3BF_4SiNi$: C, 58.49; H, 3.95; N, 7.58; Found: C, 58.41; H, 3.89; N, 7.65; IR (KBr, cm^{-1}): 2196, ν(C ≡ C); 2145, ν(C ≡ CSi); 1610, ν(C = N); 1073, ν(BF_4); UV-Vis (DMF) λ_{max} (nm) ($\varepsilon \times 10^3$, M^{-1} cm^{-1}): 243 (24.8), 278 (14.5), 366 (7.89), 535 (1.22); ^{1}H NMR (d_6-DMSO) (300 MHz): δ 8.65 (s, 1H, HC = N), 8.69–7.15 (m, 19H, Ar-H), 0.28 (s, 9H, $Si(CH_3)_3$); MS (ESI): *m/z* 652 (M-BF_4)$^+$; **6a**: Yield: 84%; Elemental analyses (C, H and N, wt%) Anal. Calc. for $C_{36}H_{29}N_4O_3PF_6SiNi$: C, 54.23; H, 3.67; N, 7.03; Found: C, 54.16; H, 3.60; N, 7.11; IR (KBr, cm^{-1}): 2194, ν(C ≡ C); 2147, ν(C ≡ CSi); 1608, ν(C = N); 843, 558, ν(P-F); UV-Vis (DMF) λ_{max} (nm) ($\varepsilon \times 10^3$, M^{-1} cm^{-1}): 249 (24.1), 281 (14.8), 372 (7.69), 527 (0.81); ^{1}H NMR (d_6-DMSO) (300 MHz): δ 8.65 (s, 1H, HC = N), 8.71–7.19 (m, 19H, Ar-H), 0.29 (s, 9H, $Si(CH_3)_3$); MS (ESI): *m/z* 652 (M-PF_6)$^+$.

Synthesis of Complex [Zn(L)(phen)]X (1b-3b)

To a solution of the appropriate Zn(II) salt, ((0.399 mmol, 0.1486 g), $Zn(ClO_4)_2·6H_2O$; (0.399 mmol, 0.0954 g), $Zn(BF_4)_2$ or (0.399 mmol, 0.1418 g), $Zn(PF_6)_2$) in THF (10 ml), an equimolar solution of ligand (**L**) (0.399 mmol, 0.175 g) in CH_2Cl_2 (20 ml) solution was added while stirring. The mixture was stirred for 20 min at room temperature. To this, a solution of one equivalent of 1, 10-phenanthroline (0.399 mmol, 0.0791 g) in THF (10 ml) was added with continuous stirring. The mixture was refluxed for 4 h. The precipitate obtained was filtered off, washed with diethyl ether and dried under vacuum.

1b: Yield: 79%; Elemental analyses (C, H and N, wt%) Anal. Calc. for $C_{38}H_{29}N_4O_7ClSiZn$: C, 58.32; H, 3.73; N, 7.16; Found: C, 58.27; H, 3.66; N, 7.23; IR (KBr, cm^{-1}): 2195, ν(C ≡ C); 2148, ν(C ≡ CSi); 1606, ν(C = N); 1096, 625, ν(ClO_4); UV-Vis (DMF) λ_{max} (nm) ($\varepsilon \times 10^3$, M^{-1} cm^{-1}): 239 (27.7), 291 (16.8), 408 (11.0); ^{1}H NMR (d_6-DMSO) (300 MHz): δ 8.65 (s, 1H, HC = N), 8.71–7.04 (m, 19H, Ar-H), 0.28 (s, 9H, $Si(CH_3)_3$); MS (ESI): *m/z* 683 (M-ClO_4)$^+$; **2b**:Yield:76%; Elemental analyses (C, H and N, wt%) Anal. Calc. for $C_{38}H_{29}N_4O_3BF_4SiZn$: C, 59.28; H, 3.80; N, 7.28; Found: C, 59.23; H, 3.74; N, 7.33; IR (KBr, cm^{-1}): 2196, ν(C ≡ C); 2146, ν(C ≡ CSi); 1608, ν(C = N); 1067, ν(BF_4); UV-Vis (DMF) λ_{max} (nm) ($\varepsilon \times 10^3$, M^{-1} cm^{-1}): 238 (28.6), 294 (16.4), 420 (11.7); ^{1}H NMR (d_6-DMSO) (300 MHz): δ 8.64 (s, 1H, HC = N), 8.68–7.10 (m, 19H, Ar-H), 0.29 (s, 9H, $Si(CH_3)_3$); MS (ESI): *m/z* 683 (M-BF_4)$^+$; **3b**: Yield: 82%; Elemental analyses (C, H and N, wt%) Anal. Calc. for $C_{38}H_{29}N_4O_3PF_6SiZn$: C, 55.11; H, 3.53; N, 6.77; Found: C, 55.07; H, 3.49; N, 6.81; IR (KBr, cm^{-1}): 2194, ν(C ≡ C); 2145, ν(C ≡ CSi); 1607, ν(C = N); 845, 558, ν(P-F); UV-Vis (DMF) λ_{max} (nm) ($\varepsilon \times 10^3$, M^{-1} cm^{-1}): 246 (27.9), 308

(16.3), 416 (10.0); ^{1}H NMR (d_6-DMSO) (300 MHz): δ 8.64 (s, 1H, HC = N), 8.73–7.15 (m, 19H, Ar-H), 0.29 (s, 9H, Si(CH$_3$)$_3$); MS (ESI): *m/z* 683 (M-PF$_6$)$^+$.

Synthesis of Complex [Zn(L)(bipy)]X (4b-6b)

To a solution of the appropriate Zn(II) salt, ((0.421 mmol, 0.1571 g), Zn(ClO$_4$)$_2$·6 H$_2$O; (0.421 mmol, 0.1008 g), Zn(BF$_4$)$_2$ or (0.421 mmol, 0.1499 g), Zn(PF$_6$)$_2$) in THF (10 ml), an equimolar quantity of **L** (0.421 mmol, 0.185 g) in CH$_2$Cl$_2$ (20 ml) was added while stirring. The mixture was stirred for 20 min at room temperature. To this, a solution of one equivalent of 2, 2′-bipyridine (0.421 mmol, 0.0659 g) in THF (10 ml) was added with continuous stirring. The mixture was refluxed for 4 h. The precipitate obtained was filtered off, washed with diethyl ether and dried under vaccum.

4b: Yield: 75%. Elemental analyses (C, H and N, wt%) Anal. Calc. for $C_{36}H_{29}N_4O_7ClSiZn$: C, 57.00; H, 3.85; N, 7.39; Found: C, 56.93; H, 3.79; N, 7.44; IR (KBr, cm^{-1}): 2195, ν(C ≡ C); 2147, ν(C ≡ CSi); 1606, ν(C = N); 1095, 623, ν(ClO$_4$); UV-Vis (DMF) λ_{max} (nm) (ε ×10^3, M^{-1} cm^{-1}): 249 (27.3), 292 (16.5), 397 (11.3) ; ^{1}H NMR (d_6-DMSO) (300 MHz): δ 8.65 (s, 1H, HC = N), 8.65–6.96 (m, 19H, Ar-H), 0.29 (s, 9H, Si(CH$_3$)$_3$), MS (ESI): *m/z* 683 (M-ClO$_4$)$^+$; **5b**: Yield: 81%; Elemental analyses (C, H and N, wt%) Anal. Calc. for $C_{36}H_{29}N_4O_3BF_4SiZn$: C, 57.97; H, 3.92; N, 7.51; Found: C, 57.91; H, 3.87; N, 7.56; IR (KBr, cm^{-1}): 2194, ν(C ≡ C); 2148, ν(C ≡ CSi); 1609, ν(C = N); 1071, ν(BF$_4$); UV-Vis (DMF) λ_{max} (nm) (ε ×10^3, M^{-1} cm^{-1}): 254 (28.4), 312 16.0), 410 (11.2); ^{1}H NMR (d_6-DMSO) (300 MHz): δ 8.65 (s, 1H, HC = N), 8.69–6.98 (m, 19H, Ar-H), 0.28 (s, 9H, Si(CH$_3$)$_3$); MS (ESI): *m/z* 683 (M-BF$_4$)$^+$; **6b**: Yield: 79%; Elemental analyses (C, H and N, wt%) Anal. Calc. for $C_{36}H_{29}N_4O_3PF_6SiZn$: C, 53.77; H, 3.64; N, 6.97; Found: C, 53.69; H, 3.61; N, 7.05; IR (KBr, cm^{-1}): 2196, ν(C ≡ C); 2145, ν(C ≡ CSi); 1610, ν(C = N); 844, 558, ν(P-F); UV-Vis (DMF) λ_{max} (nm) (ε ×10^3, M^{-1} cm^{-1}): 255 (25.5), 317 (16.1), 413 (10.6); ^{1}H NMR (d_6-DMSO) (300 MHz): δ 8.64 (s, 1H, HC = N), 8.75–7.11 (m, 19H, Ar-H), 0.28 (s, 9H, Si(CH$_3$)$_3$); MS (ESI): *m/z* 683(M-PF$_6$)$^+$.

X-Ray Crystallography

Single crystal X-ray structural study of **L** was performed on Bruker KAPPA APEX-II diffractometer. Data were collected in omega and phi scan mode, MoKα =0.71073 Å at room temperature with scan width of 0.3° at θ (0°, 90° and 180°) by keeping the distance at 40 mm between sample to fixed detector at 24°. The X-ray generator was operated at 50 kV and 30 mA. The details of crystal data, data collection and the refinements are given in Table 1. The X-ray data collection was monitored by SMART program (Bruker, 2003). All the data were corrected using SAINT and SADABS programs (Bruker, 2003). SHELX-97 was used to solution of structure and full matrix least-squares refinement on F2 [24]. Molecular and packing diagrams were generated using ORTEP-3 and Mercury-3.

Table 1 Crystal data and structure refinement details for **L**

Empirical formula	C_{26} H_{22} N_2 O_3 Si
Formula weight	438.54
Crystal system	Monoclinic
Space group	P2$_1$
a (Å)	6.0262(3)
b (Å)	7.3503 (4)
c (Å)	25.4608 (14)
α (°)	90.00
β (°)	91.266
γ (°)	90.00(3)
V (A^3)	1127.49(10)
Z	2
Density (mg/m^3)	1.292
μ (M$_0$K$_\alpha$)(mm^{-1})	0.562
F (000)	460
Data collection	
Temperature (K)	293(2)
θ mini.-maxi.(deg)	2.400 to 25.992
Data set [*h, k, l*]	-7/7,-9/9,-31/31
Total, unique data, R$_{int}$	[R(int) = 0.0641]
Observed data	>2σ(I)
Extinction coefficient	n/a
Refinement	Full-matrix least-squares on F^2
No. of reflection collected	24,414
Data / restraints / parameters	4428 / 1 / 296
R$_1$, R$_1$	0.0513, 0.0876
wR$_2$, wR$_2$	0.1187, 0.1386
Goodness-of-fit	1.046

Results and Discussion

The treatment of 5-ethynylsalicylaldehyde with 1-iodo-4-nitrobenzene in presence of PdCl$_2$(PPh$_3$)$_2$ and CuI in CH$_2$Cl$_2$/NEt$_3$ at 80 °C afforded 5-(4-nitrophenylethynyl)salicylaldehyde in good yield. Further reaction of 5-(4-nitrophenylethynyl)salicylaldehyde with 4-(trimethylsilylethynyl)aniline in THF afforded corresponding Schiff base ligand 2-{(E)-[(4-trimethylsilylethynylphenyl) imino]methyl}-4-(4-nitrophenylethynyl)phenol (**L**) in excellent yield (Scheme 1). A series of ternary complexes [Ni(**L**)(**phen/bipy**)]X (**1a-6a**) and [Zn(**L**)(**phen/bipy**)]X (**1b-6b**) were prepared by the reaction of **L** with metal(II) salt in presence of 1, 10-phenanthroline or 2, 2′-bipyridine in THF:CH$_2$Cl$_2$ (1:1) mixture (where; **phen** = 1, 10-phenanthroline; **bipy** = 2, 2′-bipyridine; X = ClO$_4$$^-$, BF$_4$$^-$, PF$_6$$^-$) (Fig. 1). The complexes prepared show a great thermal stability and are moisture insensitive in solid state. Composition and identity of all the complexes were deduced from satisfactory elemental analysis, FT-IR, UV-Vis, ^{1}H NMR, and mass spectral studies. They are freely soluble in DMF and DMSO but sparingly soluble in dichloromethane, chloroform and methanol.

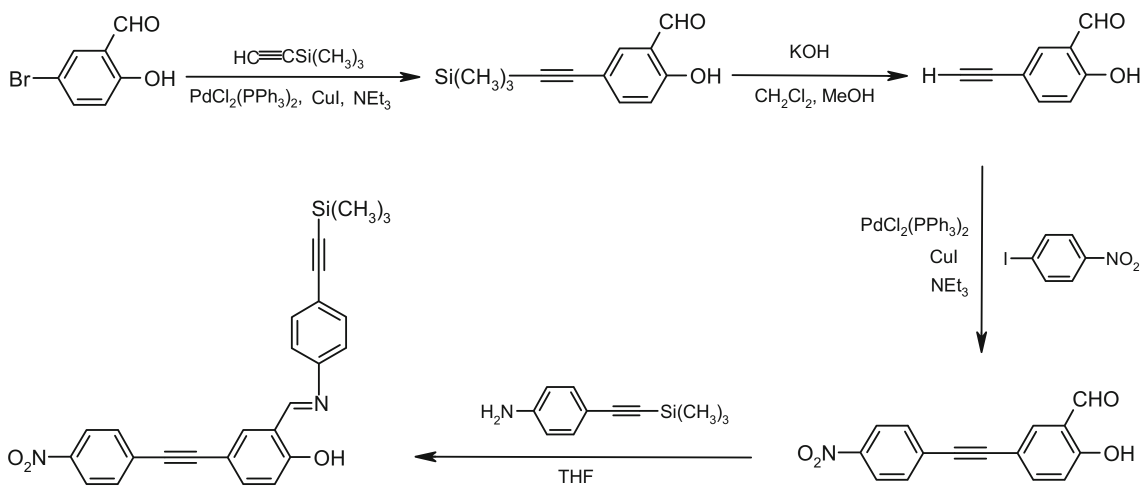

Scheme 1 Synthetic route to the preparation of L

X-Ray Structure of L

Single crystals of ligand **L** suitable for X-ray diffraction were obtained by slow evaporation of saturated solution of **L** in dichloromethane. The X-ray diffraction data was solved in the monoclinic crystal system with space group P2_1. The molecular structure of **L** along with atom numbering scheme is illustrated in Fig. 2 and the selected bond lengths and bond angles are summarized in Table 2.

The crystal and molecular structure of **L** reveals some interesting findings. First the structure exhibits a strong intramolecular (O3-H3A-N2) hydrogen bond between the nitrogen atom C = N of Schiff base and hydrogen atom of the -OH group of the salicylaldehyde ring with a distance of 147(5) Å which is in good agreement with the values reported in the literature [25]. Individually, each benzene ring in the molecule is almost planar in which the C3, C14 and C20 atom from each benzene ring has best plane by 0.042(3), 0.036(2) and 0.037(2) Å. The molecular packing of the structure is stabilized by C-H-O intermolecular hydrogen bond. All bond lengths and angles in (C1-C6), (C9-C14) and (C16-C21), benzene rings have normal values 1.376(6), 1.381(6) and 1.386(6) Å respectively. The enol form is observed in the asymmetric unit as concluded from bond lengths C15-N2 (1.273(5) Å) and C12-O3 (1.342(5) Å). The two benzene rings along with HC = N displays the trans configuration and torsion angles of N(2)-C(16)-C(17)-C(18) is 177.6(4)°, C(17)-C(16)-N(2)-C(15) is −166.8(4)° and N(2)-C(16)-C(21)-C(20) is 177.3(4)°, these angles are reported in the literature with values of −176.8(2)°, −146.7(2)° and 175.5(2)° [26]. The bond distance between C(7)-C(8) is 1.194(6) Å and C(22)-C(23) is 1.202(6) Å and Si(1)-C(23) is 1.848(4) Å are smaller due to the presence of $C \equiv CSiMe_3$. These results are comparable with those of the ligands reported earlier containing the similar moiety [27]. The ligand **L** participate in weak C(6)-H(6)-O(1) and C(2)-H(2)-O(2) hydrogen bonds with oxygen atom from nearest nitro group in the crystal lattice, at the same time it being an acceptor of such hydrogen bond through its own (O1) and (O2) atom.

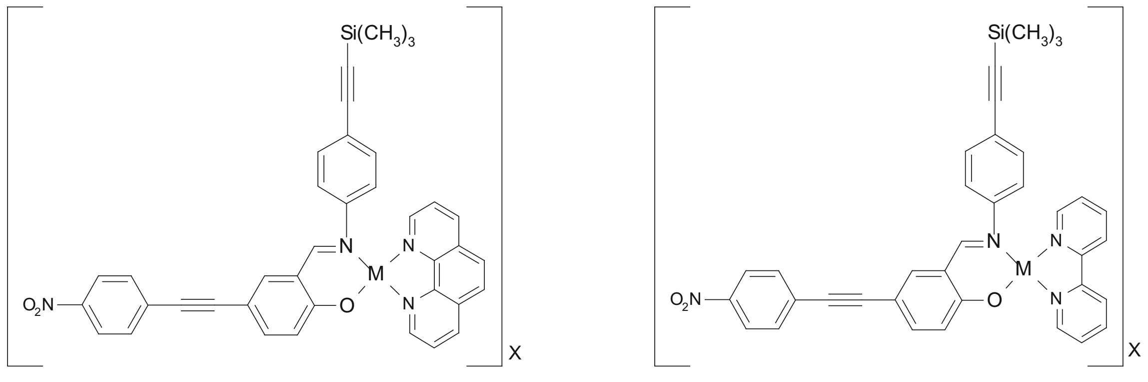

1a-3a and 1b-3b

4a-6a and 4b-6b

M= Ni(II)(**1a-6a**), Zn(II) (**1b-6b**); X= ClO_4^-, BF_4^-, PF_6^-

Fig. 1 Proposed molecular structure of the complexes **1a-6a** and **1b-6b**

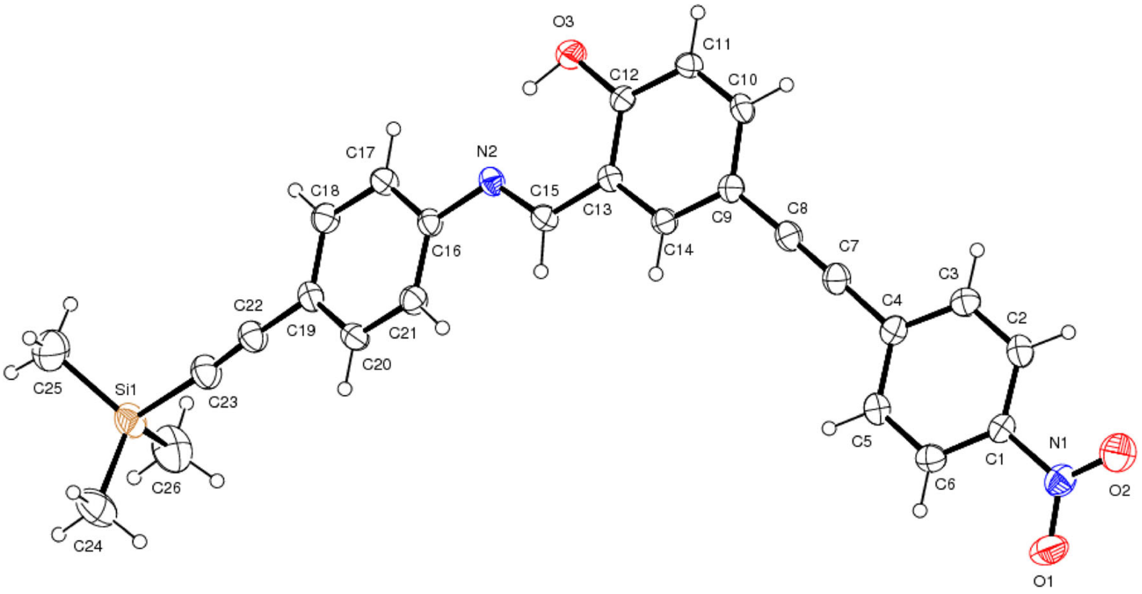

Fig. 2 Single crystal X-ray diffraction structure of L

Spectroscopic Properties

The IR spectra of selected groups in the spectra of **L** and their Ni(II) (**1a-6a**) and Zn(II) (**1b-6b**) complexes are given in section 2. In the IR spectra of **L**, a broad band at 2995 cm^{-1} assigned to ν(OH) vibration associated intramolecularly with the nitrogen atom of the CH = N group. This band disappeared in **1a-6a** and **1b-6b** confirmed the coordination of phenolic oxygen to the metal (II) centers [28]. The medium intensity band at 2203, 2155 cm^{-1} in the spectra of **L** undergo smaller deshielding in all Ni(II) and Zn(II) complexes. Along with this band the ligand **L** and its **1a-6a** and **1b-6b** complexes exhibit vibrations of Me_3Si at around 1248 and 840 cm^{-1}. Another band at 1618 cm^{-1} observed in the spectra of **L** slightly shifted towards lower frequency at 1608 cm^{-1} for **1a-6a** and 1607 cm^{-1} for **1b-6b**. This change in frequency indicating imine nitrogen coordination. The characteristic band appeared at 1287 cm^{-1} in **L** attributed to the phenolic stretch. This band observed at lower wave number by ca 10–20 cm^{-1} in the spectra of **1a-6a** and **1b-6b** relative to **L** suggesting involvement of the C-O moiety in coordination. In addition, bands at ca 1500, 800 and 730 cm^{-1} in the phenanthroline complexes and 760, 740 cm^{-1} in the bipyridine complexes confirm the coordination of these ligand in the complexes. The perchlorate complexes **1a**, **1b** and **4a**, **4b** exhibit typical bands in expected regions; broad band at ~1096 cm^{-1} (ν_3) and strong band at ~624 cm^{-1} (ν_4) are due to stretching vibration of non-coordinated ClO_4^- ion [29]. A broad band at around 1069 cm^{-1} in **2a** and **5a** and 1072 cm^{-1} in **2b** and **5b** corresponds to the presence of BF_4^- anion. However, existence of PF_6^- ion is exhibited by intense and medium bands occurring at ~844 and ~558 cm^{-1}, respectively confirming formation of complexes **3a**, **3b**, **6a** and **6b** [30].

Table 2 Selected bond lengths (Å) and bond angles (°) for **L**

Bond lengths (Å)		Bond angles (°)	
C(7)-C(8)	1.194(6)	O(1)-N(1)-O(2)	123.2(4)
C(22)-C(23)	1.202(6)	O(1)-N(1)-C(1)	118.0(4)
C(1)-N(1)	1.466(5)	O(2)-N(1)-C(1)	118.7(4)
N(1)-O(1)	1.212(5)	C(15)-N(2)-C(16)	120.7(4)
N(1)-O(2)	1.213(5)	C(25)Si(1)-C(24)	110.6(4)
C(12)-O(3)	1.342(5)	C(25)Si(1)-C(23)	106.8(3)
C(15)-N(2)	1.273(5)	C(24)Si(1)-C(23)	109.0(3)
C(16)-N(2)	1.429(5)	C(25)Si(1)-C(26)	111.4(3)
Si(1)-C(23)	1.848(4)	C(24)Si(1)-C(26)	109.8(3)
Si(1)-C(24)	1.847(7)	C(23)Si(1)-C(26)	109.1(3)
Si(1)-C(25)	1.838(6)		
Si(1)-C(26)	1.851(6)		

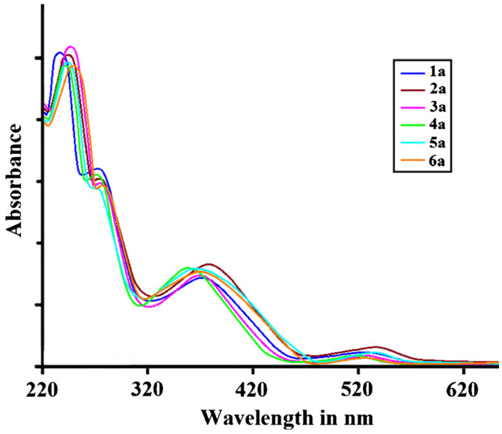

Fig. 3 Electronic Absorption Spectra of complexes **1a-6a**

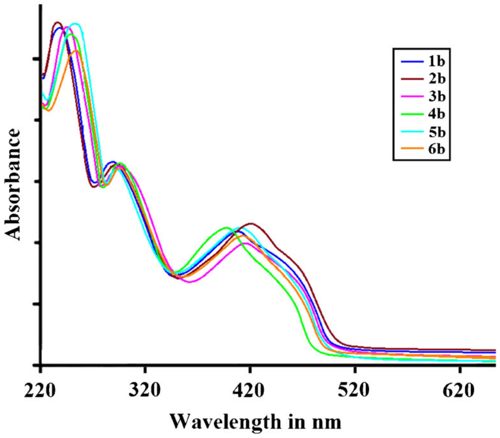

Fig. 4 Electronic Absorption Spectra of complexes **1b-6b**

The UV-visible absorption spectra of **L** and its Ni(II) **(1a-6a)** and Zn(II) (**1b-6b)** complexes were measured in dimethylformamide solution (10^{-4} M) at room temperature and data are summarized in section 2. The absorption spectra of **L** exhibit two intense bands at 231 and 265 nm which may associated with π → π* and n → π* intraligand transitions, respectively. Analogous bands are also observed in the complexes at 235–249 and 274–281 nm for Ni(II) (**1a-6a)** (Fig. 3) and 238–255 and 291–317 nm for Zn(II) (**1b-6b**) (Fig. 4) complexes. The observed bathochromic shift in these complexes relative to **L** is in accordance with coordination of **L** to the metal ion. The low energy transition located at 359–376 nm in **1a-6a** and 397–420 nm in **1b-6b** are attributed to the metal to ligand charge transfer (MLCT) transition. In addition to these bands a weak absorption at 525–536 nm in **1a-3a** and 518–535 nm in **4a-6a** presumably due to spin allowed ($^1A_{1g} \rightarrow {}^1A_{2g}$) d-d transition for Ni(II) in square planar geometry [31]. Low value of d-d transition observed in **phen** complexes (**1a-3a** and **1b-3b**) indicating that in these complexes the basal planes are comparatively more distorted than **bipy** complexes (**4a-6a** and **4b-6b**).

The ^{1}H NMR spectra of **L** showed two characteristics resonances, first at ~δ 13.29 ppm corresponding to the phenolic -OH proton and another at ~δ 8.61 ppm assigned to the imine (CH = N) proton. After coordination to Ni(II) and Zn(II) along with **phen** or **bipy** the resonance for phenolic protons get disappeared in the spectra of **1a-6a** and **1b-6b** indicating deprotonation of **L** and coordination of phenolic oxygen to the metal ion [32]. The imine proton shifted to downfield region and observed at around δ 8.65 ppm in **1a-6a** and δ 8.64 ppm in **1b-6b** confirm the coordination through imine nitrogen [33]. The ^{1}H NMR spectra shows several coupled multiplets along with additional peaks in the aromatic region at δ 6.90–8.71 ppm for **1a-6a** and δ 6.96–8.75 ppm for **1b-6b** associated with coordinated **phen** or **bipy** ligand along with ring protons of **L**. However, a sharp singlet at δ 0.27 ppm in **L** due to terminal $SiMe_3$ remains unchanged in **1a–6a** and **1b–6b.**

Thermogravimetric Analysis

The thermal behavior of Ni(II) (**1a-6a**) and Zn(II) (**1b-6b**) complexes were studied by thermogravimetric (TG) analysis in the range 25 to 800 °C under flowing nitrogen at a heating rate of 10 °C min^{-1}. The perchlorate complexes **1a**, **4a**, **1b** and **4b** are potentially explosive and hence are not studied for safety reason. All Ni(II) and Zn(II) complexes are stable up to 180–225 °C, indicating that these complexes do not undergo mass loss of water or other solvent molecule. The thermal decomposition process of **2a-6a** and **2b-6b** involves two decomposition stages. The TGA plot of complexes **2a**, **3a**, **2b** and **3b** shows the first decomposition stage is assigned to the decomposition of coordinated salicylidene ligand **L** and takes place in the region 180–525 °C (**2a**), 198–519 °C (**3a**), 210–538 °C (**2b**) and 218–532 °C (**3b**) corresponding to mass loss of 56.99%, 52.93%, 56.61% and 52.49%, respectively (theoretical mass loss 57.32% (**2a**), 53.26% (**3a**), 56.82% (**2b**) and 52.83% (**3b**)). The second decomposition stage occurs between 525–728, 519–714, 538–740 and 532–735 °C corresponds to mass loss of 25.61% (**2a**), 23.88% (**3a**), 25.56% (**2b**) and 23.67% (**3b**), respectively attributed to the decomposition of coordinated 1, 10-phenanthroline leaving $NiBF_4$, $NiPF_6$ and $ZnBF_4$, $ZnPF_6$ as final residue (theoretical mass loss 25.97% (**2a**), 24.13% (**3a**), 25.74% (**2b**) and 23.93% (**3b**)). The complexes **5a**, **6a**, **5b** and **6b** show very similar behavior to the above, once again the complexes undergo a

Table 3 Electrochemical data of Ni(II) complexes (**1a-6a**) in dimethylformamide (10^{-4} M)

Compound	Oxidation potentials			Reduction potentials		
	E_{pa}(V)	E_{pc}(V)	$E_{1/2}$(V) ΔE_p(mV)	E_{pa}(V)	E_{pc}(V)	$E_{1/2}$(V) ΔE_p(mV)
1a	1.298	1.123	1.211(175)	-1.107	-1.245	-1.176(138)
2a	1.391	1.135	1.263(256)	-1.152	-1.369	-1.260(217)
3a	1.265	1.104	1.184(161)	-1.139	-1.347	-1.243(208)
4a	1.193	1.021	1.107(172)	-1.184	-1.292	-1.238(108)
5a	1.227	0.989	1.108(238)	-1.249	-1.325	-1.287(76)
6a	1.164	0.957	1.065(207)	-1.221	-1.274	-1.247(53)

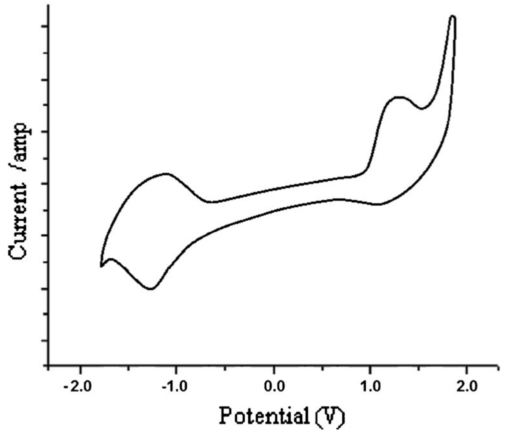

Fig. 5 Cyclic voltammogram of **1a**

significant weight loss of 58.89% (**5a**), 54.72% (**6a**), 58.52% (**5b**) and 54.31% (**6b**) in the temperature range 184–529 (**5a**), 193–515 (**6a**), 207–542 (**5b**) and 220–551 °C (**6b**) is assigned to the decomposition of coordinated salicylidene ligand **L** (theoretical mass loss. 59.19% (**5a**), 54.87% (**6a**), 58.65% (**5b**) and 54.41% (**6b**) respectively), while the second decomposition stage occurs in the temperature range 529–722 (**5a**), 515–726 (**6a**), 542–739 (**5b**) and 551–732 °C (**6b**), indicative of gradual breakdown of coordinated 2, 2′-bipyridine (observed weight loss of 21.01%, 19.49%, 20.87% and 19.36%; theoretical mass loss of 21.12% (**5a**) and 19.59% (**6a**), 20.96% (**5b**) and 19.42% (**6b**)) leaving $NiBF_4$, $NiPF_6$, $ZnBF_4$ and $ZnPF_6$ as a final residue.

Electrochemical Studies

The electrochemical behaviour of Ni(II) complexes (**1a-6a**) were studied by cyclic voltammetry in dimethylformamide solution (10^{-4} M) containing 0.05 M n-Bu_4NClO_4 as supporting electrolyte. The electrochemical data are presented in Table 3 and cyclic voltammogram of representative complexes **1a** and **5a** are shown in Figs. 5 and 6, respectively.

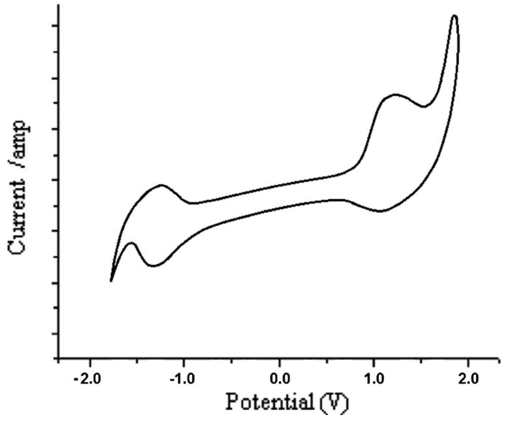

Fig. 6 Cyclic voltammogram of **5a**

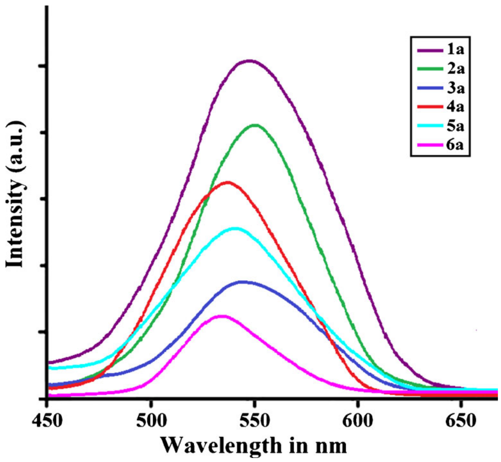

Fig. 7 Emission spectra of complexes **1a-6a**

All the Ni(II) complexes exhibit both anodic and cathodic redox potentials. In anodic potential region the reduction wave (Epc, 0.957–1.135 V) corresponding to Ni(III)/Ni(II) reaction is obtained. During the reverse scan the oxidation of Ni(II)/Ni(III) occurs in the potential range (Epa, 1.164–1.391 V). In cathodic potential region the reduction wave (Epc, −1.245 to −1.369 V) corresponding to Ni(II)/Ni(I) reaction is obtained. During the reverse scan the oxidation of Ni(I)/Ni(II) occurs in the potential range (Epa, −1.107 to −1.249 V). However the values of the limiting peak-to-peak separation (ΔEp) ranging from 53 to 256 mV reveal that this process can be quasireversible. Further, the redox process among the mixed ligand Ni(II) complexes of **phen** appears at more positive potential (1.184–1.263 V) as compared to those for corresponding **bipy** complexes (1.065–1.108 V). This trend may be due to good stabilization of the **phen** complexes compared to the **bipy** complexes, as a result of its strong π-acidic character. These results are in close agreement with those reported in the literature [34].

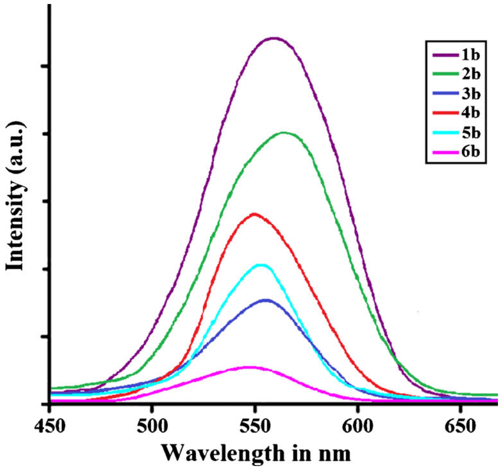

Fig. 8 Emission spectra of complexes **1b-6b**

Emission Behavior

The emission spectra of the ligand **L** and its Ni(II) (**1a-6a**) and Zn(II) (**1b-6b**) complexes were explored in dimethylformamide solution (10^{-4} M). The emission spectra of **1a-6a** and **1b-6b** are depicted in Figs. 7 and 8 and data are collected in Table 4. The ligand **L** exhibit emission in the green region centered at λ_{max} = 488 nm with an excitation at λ_{max} = 330 nm attributed to emission due to ligand centered π–π^* electron transition. In contrast, all the Ni(II) and Zn(II) complexes show steady state marked differences in emission behaviour in DMF solution. The emission spectra of **1a-3a** and **4a-6a** show broad emission spectra with emission maxima at 545–550 nm in **1a-3a** and 535–541 nm in **4a-6a** upon excitation at 335–346 and 345–355 nm, respectively. The emission spectra of **1b-3b** and **4b-6b** bathochromically shifted at longer wavelength with high intensity and exhibit emission at 558–565 and 548–555 nm upon excitation at 320–330 and 340–350 nm, respectively. The emission observed in these complexes reveals that the emission origin predominantly due to $\pi \rightarrow \pi^*$ intra-ligand. Compare to **L** the significant bathochromic shift in the emission spectra of Ni(II) and Zn(II) complexes confirm the chelation of **L** to metal(II) ion which effectively increases the ligand conformational rigidity and thus reducing the non-radiative loss [35]. It was observed that the fluorescence efficiency of the **phen** complexes (**1a**–**3a** and **1b-3b**) appears at longer wavelength with enhanced intensity as compared to **bipy** (**4a-6a** and **4b–6b**) complexes (Table 4). This is might be due to non-radiative decay process which is more effective in the **bipy** complexes as compared to **phen** complexes. It was also observed that the emission energy of the Ni(II) and Zn(II) complexes is sensitive to size of the counter anion (Table 4). When the size of the counter-anion increases the emission wavelength of all the complexes decreases and emission energy follows the sequence BF_4^-<ClO_4^-<PF_6^-. These results could be attributed to difference in coordinating ability of BF_4^-, ClO_4^-, and PF_6^- with metal ion as well as difference in solubility of the complexes in solution [36].

The fluorescence quantum yield (ϕ) of all complexes was determined with reference to quinine sulphate (ϕ = 0.52) and observed at 0.1845–0.2413 for **1a-6a** and 0.4595–0.5381 for **1b-6b**. The area of the emission spectrum was integrated using the software available on the instrument and the quantum yields were calculated according to the following equation.

$$\frac{\varphi_S}{\varphi_R} = \frac{[A_S]}{[A_R]} X \frac{[(Abs)_R]}{[(Abs)_S]} X \frac{[\eta_S^2]}{[\eta_R^2]}$$

Here ϕ_S and ϕ_R are the fluorescence quantum yield of the sample and reference, respectively. A_S and A_R are the areas under the fluorescence spectra of the sample and reference, respectively, $(Abs)_S$ and $(Abs)_R$ are the respective optical densities of the sample and the reference solution at the wavelength of excitation and η_s and η_R are the values of refractive index for the respective solvent used for the sample and reference. The significant increase in ϕ value is observed for **1a-3a** and **1b-3b** as compared to **4a-6a** and **4b-6b.** These results might be due to better coordination of ligands to Ni(II) and Zn(II). The Life time data of all the compounds are taken at 298 K in DMF solution when excited at 320 nm. The observed decay of the complexes fit well with mono exponential nature of the complexes and found to be 2.58–3.38 ns for **1a-6a** and 3.38–4.32 ns for **1b-6b** (Table 4**)**. Compare to **1a-6a** the average lifetime of **1b-6b** is longer than those observed for **1a-6a**. These results could be attributed to red shifted emission and increased emission intensity observed in **1b-6b** compare to **1a-6a**.

Table 4 Emission data of Nickel (II) (1a-6a) and Zn(II) (1b-6b) complexes in dimethylformamide

Complex	λ_{ex} (nm)	λ_{em} (nm)	ϕ	τ (ns)	K_r ($s^{-1}/10^9$)	K_{nr} ($s^{-1}/10^9$)
1a	335	547	0.2362	2.99	0.07899	0.2554
2a	340	550	0.2413	3.38	0.07139	0.2244
3a	346	545	0.2081	2.74	0.07595	0.2890
4a	345	537	0.1950	2.69	0.07249	0.2992
5a	350	541	0.2174	3.16	0.06879	0.2476
6a	355	535	0.1845	2.58	0.07147	0.3161
1b	320	560	0.4976	3.91	0.1272	0.1285
2b	325	565	0.5381	4.32	0.1245	0.1069
3b	330	558	0.4835	3.84	0.1259	0.1345
4b	340	550	0.4792	3.46	0.1385	0.1505
5b	345	555	0.4923	4.11	0.1197	0.1236
6b	350	548	0.4595	3.38	0.1359	0.1599

Conclusion

In present study some nickel(II) and zinc(II) complexes of the type [Ni(**L**)(**phen**/**bipy**)]X(**1a–6a**) and [Zn(**L**) (**phen**/**bipy**)]X (**1b–6b**) (where **L** = 2-{(E)-[(4-trimethylsilylethynylphenyl)imino]methyl}-4-(4-nitrophenylethynyl)phenol; **phen** = 1, 10-phenanthroline, **bipy** = 2,2-bipyridine; X = ClO_4^-, BF_4^-, PF_6^-) have been prepared and characterized. All Ni(II) complexes exhibit both positive and negative redox potential corresponding to Ni(II)/Ni(III) and Ni(II)/Ni(I) process, respectively. Further, the redox processes of Ni(II)-phenanthroline complexes appears at more positive potential as compared to those for corresponding bipyridine complexes. The room temperature luminescence is observed for all complexes in DMF solution as a result of $\pi \rightarrow \pi^*$ ILCT transition. The size of the counter anion and heterocyclic coligands **phen** and **bipy** shows pronounced effect on emission properties of the complexes.

Acknowledgements We gratefully acknowledge Head, Sophisticated Analytical Instrument Facility Center, IIT, Madras, India for providing single crystal X-ray facilities.

References

1. Andruh M (2011) Compartmental Schiff-base ligands—a rich library of tectons in designing magnetic and luminescent materials. Chem Commun 47:3025–3042
2. Schull TL, Kuchmerick JG, Patterson CH, George C, Moore MH, Pollack SK, Shashidhar R (2003) Ligand effects on charge transport in platinum(II) Acetylides. J Am Chem Soc 125:3202–3203
3. Ho KY, Yu WY, Cheung KK, Che CM (1999) Blue luminescent zinc(II) complexes with polypyridylamine ligands: crystal structures and luminescence properties. J Chem Soc Dalton Trans: 1581–1586
4. Lacroix PG (2001) Second-order optical nonlinearities in coordination chemistry: the case of bis(salicylaldiminato)metal Schiff Base complexes. Eur J Inorg Chem 2:339–348
5. Garoufis A, Hadjikakou SK, Hadjiliadis N (2009) Palladium coordination compounds as anti-viral, anti-fungal, anti-microbial and anti-tumor agents. Coord Chem Reviews 253:1384–1397
6. Shi Q, Xu L, Ji J, Li Y, Wang R, Zhou Z, Cao R, Hong M, Chan ASC (2004) Syntheses and structures of two anion-templated dinuclear cadmium complexes with diamino-binaphthyl Schiff bases as ligands. Inorg Chem Commun 7:1254–1257
7. Ziessel R (2001) Schiff-based bipyridine ligands. Unusual coordination features and mesomorphic behaviour. Coord Chem Reviews 216–217:195–223
8. Golcu A, Tumer M, Demirelli H, Wheatley RA (2005) Cd(II) and Cu(II) complexes of polydentate Schiff base ligands: synthesis, characterization, properties and biological activity. Inorg Chimi Acta 358:1785–1797
9. Bella SD, Oliveri IP, Colombo A, Dragonetti C, Righettob S, Roberto D (2012) An unprecedented switching of the second-order nonlinear optical response in aggregate bis (salicylaldiminato)zinc(II) Schiff-base complexes. Dalton Trans 41:7013–7016
10. Oliveri IP, Failla S, Malandrinoa G, Bella SD (2011) New molecular architectures by aggregation of tailored zinc(II) Schiff-base complexes. New J Chem 35:2826–2831
11. Zhou L, Cai P, Feng Y, Cheng J, Xiang H, Liu J, Wu D, Zhou X (2012) Synthesis and photophysical properties of water-soluble sulfonato-salen-type Schiff bases and their applications of fluorescence sensors for Cu^{2+} in water and living cells. Anal Chim Acta 735:96–106
12. Consiglio G, Failla S, Finocchiaro P, Oliveri IP, Bella SD (2012) Aggregation properties of bis(salicylaldiminato)zinc(II) Schiff-base complexes and their Lewis acidic character. Dalton Trans 41:387–395
13. Hai Y, Chen J-J, Zhao P, Lv H, Yu Y, Xu P, Zhang J-L (2011) Luminescent zinc salen complexes as single and two-photon fluorescence subcellular imaging probes. Chem Commun 47:2435–2437
14. Sano T, Nishio Y, Hamada Y, Takahashi H, Usuki T, Shibata K (2000) Design of conjugated molecular materials for optoelectronics. J Mater Chem 10:157–161
15. Averseng F, Lacroix PG, Malfant I, Dahana F, Nakatani K (2000) Synthesis, crystal structure and solid state NLO properties of a new chiral bis(salicylaldiminato)nickel(II) Schiff-base complex in a nearly optimized solid state environment. J Mater Chem 10:1013–1018
16. Nielsen M, Larsen NB, Gothelf KV (2002) Electron transfer reactions of self-assembled monolayers of Thio(Phenylacetylene)$_n$-substituted chiral metal-salen complexes. Langmuir 18:2795–2799
17. Schmitz C, Pösch P, Thelakkat M, Schmidt H-W, Montali A, Feldman K, Smith P, Weder C (2001) Polymeric light-emitting diodes based on poly(p-phenyleneethynylene), poly(triphenyl diamine) and Spiroquinoxaline. Adv Funct Mater 11:41–46
18. Liuzzo V, Oberhauser W, Pucci A (2010) Synthesis of new red photoluminescent Zn(II)-salicylaldiminato complex. Inorg Chem Commun 13:686–688
19. Wallenhorst C, Kehr G, Luftmann H, Frohlich R, Erker G (2008) Bis(iminoethyl)pyridine systems with a pendant alkenyl group part a: cobalt and iron complexes and their catalytic behavior. Organometallics 27:6547–6556
20. Sunatsuki Y, Motoda Y, Matsumoto N (2002) Copper(II) complexes with multidentate Schiff-base ligands containing imidazole groups: ligand-complex or self-complementary molecule. Coord Chem Reviews 226:199–209
21. Sousa C, Gameiro P, Freire C, de Castro B (2004) Nickel(II) and copper(II) Schiff base complexes bearing benzo-15-crown-5 functionalities as probes for spectroscopic recognition of lanthanide ions. Polyhedron 23:1401–1408
22. More MS, Pawal SB, Lolage SR, Chavan SS (2017) Syntheses, structural characterization, luminescence and optical studies of Ni(II) and Zn(II) complexes containing salophen ligand. J Mol Str 1128:419–427
23. Ardizzoia GA, Brenna S, Durini S, Theirrien B (2015) Synthesis and characterization of luminescent zinc(II) complexes with a N,N-bidentate 1-pyridylimidazo[1,5-a]pyridine ligand. Polyhrdron 90: 214–220
24. Sheldrick GM (2008) A short history of SHELX. Acta Cryst A 64: 112–122
25. Dal H, Suzen Y, Sahin E (2007) Synthesis, spectral studies of salicylidine-pyridines: crystal and molecular structure of 2-[(1*E*)-2-aza-2-(5-methyl(2-pyridyl)ethenyl)]-4-bromobenzen-1-ol. Spectrochim Acta Part A 67:808–814
26. Ikiz M, Ispir E, Aytar E, Ulusoy M, Karabug S, Aslantas M, Celik O (2015) Chemical fixation of CO_2 into cyclic carbonates by azo-containing Schiff base metal complexes. New J Chem 39:7786–7796
27. Ziessel R (1996) General method for the preparation of alkyne-functionalized Oligopyridine building blocks. J Org Chem 61: 6535–6546
28. TuÈmer M, Seyin H, Ksal K, Serin S, Digrak M (1999) Antimicrobial activity studies of mononuclear and binuclear

mixed-ligand copper(II) complexes derived from Schiff base ligands and 1,10-phenanthroline. Transit Met Chem 24:13–17

29. Mukherjee A, Chakrabarty R, Ng SW, Patra GK (2010) The syntheses, characterizations, X-ray crystal structures and properties of Cu(I) complexes of a bis-bidentate schiff base ligand. Inorg Chimi Acta 363:1707–1712
30. Yang R-N, Sun Y-A, Hou Y-M, Hu X-Y, Jin D-M (2000) Synthesis and reactivity of the copper(I) complex containing bis(diphenylphosphino) methane bridging ligands — structure of $[Cu_4(\mu_4\text{-}S)(dppm)_4]$ $(PF_6)_2 \cdot CH_2Cl_2$. Inorg Chimi Acta 304:1–6
31. Jonh A, Katiyar V, Pang K, Shaikh MM, Nanavati H, Ghosh P (2007) Ni(II) and Cu(II) complexes of phenoxy-ketimine ligands: synthesis, structures and their utility in bulk ring-opening polymerization (ROP) of L-lactide. Polyhedron 26:4033–4044
32. Ghaffari A, Behzad M, Pooyan M, Rudbari HA, Bruno G (2014) Crystal structures and catalytic performance of three new methoxy substituted salen type nickel(II) Schiff base complexes derived from meso-1,2-diphenyl-1,2-ethylenediamine. J Mol Struct 1063:1–7
33. Begum MS, Zangrando E, Howlader MBH, Sheikh MC, Miyatake R, Hossain MM, Alam MM, Hasnat MA (2016) Synthesis, characterization, photoluminescence and electrochemical studies of Ni^{II}, Cu^{II}, Zn^{II}, Cd^{II} and Pd^{II} complexes of the bidentate S-hexyl-β-N-(2-thienyl) methylenedithiocarbazate ligand. Polyhedron 105:56–61
34. Eggleston MK, McMillin DR, Koenig KS, Pallenberg A (1997) Steric effects in the ground and excited states of $Cu(NN)2^+$ systems. J Inorg Chem 36:172–176
35. Roy S, Sarkar BN, Bhar K, Satapathi S, Mitra P, Ghosh BK (2013) Syntheses, structures and luminescence behaviors of zinc(II) complexes containing a tetradentate Schiff base: variation in nuclearity and geometry with th change of halide/ pseudohalide/ carboxylate and counter anion. J Mol Struct 1037:160–169
36. Zhu Y, Ma Y, Zhu J (2013) The counter anion effect of ion-type phosphorescent dye tris(4,7-diphenyl-1,10-phenanthroline)ruthenium(II) complexes as dopant for light-emitting diodes. J Luminescence 137:198–203